KSME

Springer

Journal of Mechanical Science and Technology 34 (6) 2020

Original Article
DOI 10.1007/s12206-020-0534-4

Keywords:
· Lower limb exoskeleton
· Variable stiffness actuator
· Variable damping actuator
· Magneto-rheological brake
· Hybrid actuator
· Walking trajectory tracking

Correspondence to:
Ozgur Baser
ozgurbaser@sdu.edu.tr

Citation:
Baser, O., Kizilhan, H., Kilic, E. (2020). Employing variable impedance (stiffness/damping) hybrid actuators on lower limb exoskeleton robots for stable and safe walking trajectory tracking. Journal of Mechanical Science and Technology 34 (6) (2020) 2597~2607.
http://doi.org/10.1007/s12206-020-0534-4

Received September 11th, 2019
Revised March 9th, 2020
Accepted March 30th, 2020

† Recommended by Editor
Ja Choon Koo

Employing variable impedance (stiffness/damping) hybrid actuators on lower limb exoskeleton robots for stable and safe walking trajectory tracking

Ozgur Baser, Hasbi Kizilhan and Ergin Kilic

Department of Mechanical Engineering, Suleyman Demirel University, Isparta, Turkey

Abstract Compliant actuators are employed in exoskeleton robots instead of stiff actuators for safe human-robot interaction. In parallel with this idea, we previously constructed a biomimetic compliant exoskeleton robot (BioComEx). In this study, to provide more stable and safe trajectory tracking even under disturbances, magneto-rheological (MR) brakes were added to all joints of BioComEx as variable damping actuators and a PID+D controller was proposed. To evaluate the robot and controller, first, BioComEx was hung on a platform and the controller was applied without device user under external forces. This primary test results showed that the proposed design and controller can effectively minimize disturbance effects and consequently reduce trajectory tracking oscillations. In the rest of the study, the similar control experiments were repeated with a user who has unilateral lower limb movement disorders. In these experiments, the movements of the user's healthy leg were detected by force feedback impedance control algorithm and then were used as reference for the impaired leg with walking cycle delay in real time. The secondary test results showed that the variable impedance exoskeleton robot design with PID+D controller can ensure effective walking assistance for the impaired human legs.

1. Introduction

Exoskeleton robots are used in many applications such as power augmentation, rehabilitation and walking assistant [1-3]. Power augmentation robots allow the transport of heavy loads with low muscle strength [4], rehabilitation robots improve musculoskeletal function of paralyzed patients [5], and assistive robots provide walking assistance to the elderly or patients [6, 7]. The various design and control architectures of these robots were summarized in the relevant references [8, 9]. In recent years, the use of compliant actuators instead of stiff actuators has greatly increased in the exoskeletons to provide a safe human-robot interaction [10]. The compliance in these actuators is usually provided by adding elastic elements such as springs [11, 12]. It is seen that these types of actuators are used in the design of RoboKnee [13], IHMC [14] and LOPES [15, 16] robots.

The nervous-musculoskeletal system of human legs constantly changes the stiffness and damping of all joints during a gait cycle. Flexible and stable walking can thus be achieved with minimum energy consumption. Therefore, variable stiffness actuators have been introduced for biped robots by some research groups [17-19]. These actuators are used as motion units in the knee and ankle joints of exoskeleton robots such as ALTACRO [20], UVSHA [21], ATLAS [22] and XoR [23]. Besides, Enoch et al. [24] designed a bipedal robot called BLUE with variable stiffness and damping feature. The authors used directly electric motors for damping in their study. However, the direct use of electric motors in human-robot interfaces might injure the users if the device was unstable. For safety reasons, the use of electric motors alone should be avoided in human-robot interaction.

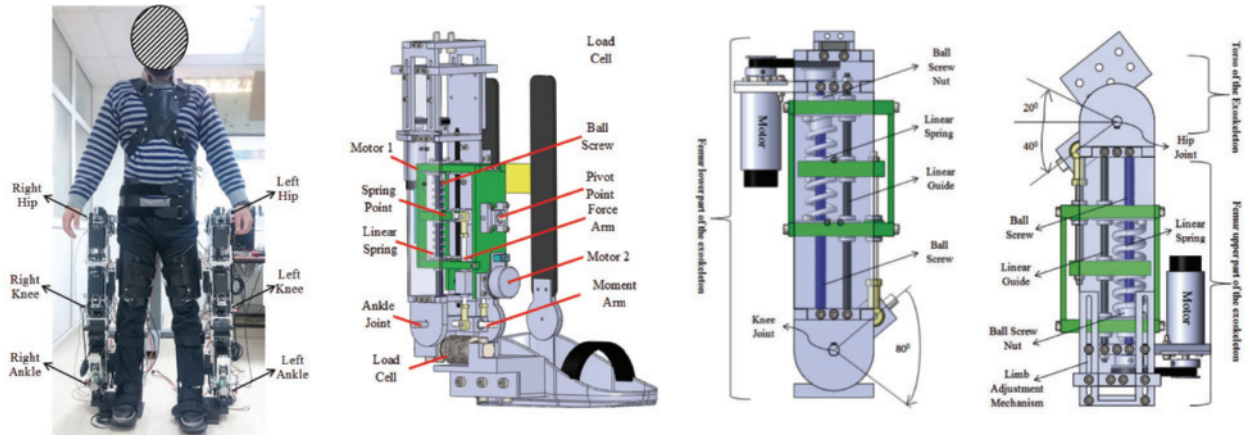

(a) (b) (c) (d)

Fig. 1. (a) BioComEx; (b) VSA design for ankle joint; (c) SEA design for knee joint; (d) SEA design for hip joint.

Our previous study [25] constructed a lower limb exoskeleton robot named BioComEx. In this design, one variable stiffness actuator (VSA) for the ankle and two series elastic actuators (SEA) for knee and hip joints were developed. The presence of elastic elements in the joints of robot causes oscillations especially under disturbance effects, which worsens system stability and risks the safety of human-robot interaction. In this study, MR brakes [26] were adapted to BioComEx's joints to achieve more stable mobility. Hence, an exoskeleton having hybrid actuators in all joints has been proposed. In the literature, there are some motion systems including hybrid actuators [27, 28]. However, these hybrid actuator designs have not previously been tested in lower limb exoskeleton robots. The primary contribution of this paper is that it is the first study in the literature which uses both a compliant actuator and MR brake in all joints of a lower limb exoskeleton. Any second order nonlinear dynamical systems like exoskeleton joints can be stabilized by the PID controller with fixed controller parameters so long as the nonlinearity satisfies a Lipschitz condition [29]. However, to achieve more stable mobility even under disturbance, a PID+D control algorithm integrated with MR brake was developed and implemented on BioComEx joints. The control structure of PID+D used here is based on the proposed control rule in Ref. [30] which was implemented on stiff actuators. There are some studies that employ PI+D control algorithms for hybrid actuators in the Ref. [31]. D controller in this technique controls only MR brake. However, the response of MR brakes is slower than active motors. The purpose of PID+D control algorithm used in this study is to achieve a faster and a stable response. That is, one D controller on the MR brake improves the stability and the other D controller on the electric motor increases the response speed. This is the second contribution of this paper. Besides, a sliding PID+D control method was used for the variable stiffness actuator in the ankle joint of BioComEx since the variable stiffness actuators require various PID parameters for different stiffness values. This is the last contribution of the paper.

To show the performance of hybrid actuators and PID+D controller, first, sinusoidal trajectory tracking experiments under external disturbances were performed without a user. Then, the walking trajectory tracking experiments were conducted with a user who had unilateral lower limb movement disorders.

This paper is organized such that after introducing the design of BioComEx and integration of MR brakes into the system, the proposed control architecture, experiments, results and discussions are presented.

2. Design of BioComEx and integration of MR brakes to robot joints

Exoskeleton robots should be designed according to the anthropomorphic configuration of human body [32, 33]. However, since increasing the degree of freedom makes the design very complex, a pseudo-anthropomorphic architecture is preferred for BioComEx. Therefore, BioComEx was developed considering the rotation of the lower limb joints only in the sagittal plane. Fig. 1 shows the design of BioComEx, which has six degrees of freedom (three DOFs per each leg). These degrees of freedom show the flexion and extension movements of the ankle, knee and hip joints in the sagittal plane. To maximize the safety of human-robot interaction and to use the robot in force feedback control studies, seven different force sensors which are independent from each other were added to each segment of the robot. For a compact design, the ankle actuator is embedded in the shank alignment of the exoskeleton robot, while the knee and hip actuators are embedded as a whole at the thigh.

Another consideration that should be taken into account in the exoskeleton design is the functionality of the joints. Therefore, before starting the joint designs, biomechanics studies of human joints in the literature were reviewed. Recently, the concept of quasi-stiffness has been explored to characterize the spring-like behavior of lower limb joints [34-36]. The quasi-stiffness is defined as the stiffness of a spring that best mimics the overall behavior of a joint during a locomotion task. It can

Table 1. Specifications of 4-pole MR brake.

Parameter	Value
Outer diameter [mm]	56
Maximum current value [A]	1
Torque/volume ratio	6.567
Maximum torque [Nm]	5
Weight [kg]	0.97
Length [mm]	85

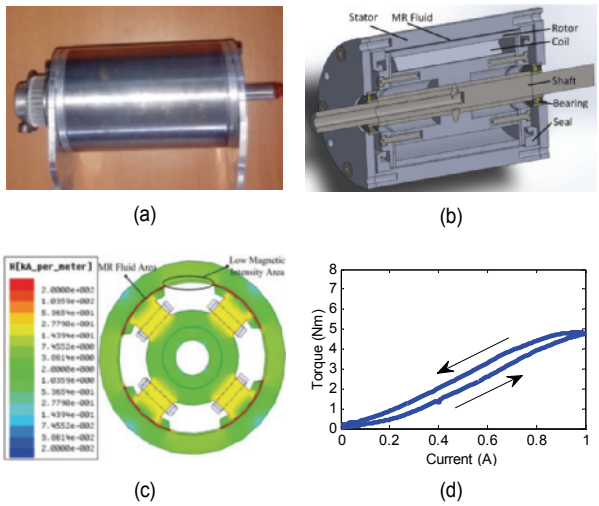

Fig. 2. (a) 4-pole MR brake; (b) cross-sectioned CAD view; (c) magnetic field strength; (d) torque-current graph [26].

be estimated using the slope of the best linear fit on the moment-angle graph of the joint [34-36]. Based on this idea, Shamaei et al. demonstrated stiffness estimations of the lower limb joints in the stance phase of the gait [37-39]. They concluded that the stiffness of the ankle needs to be changed during a gait cycle in order to obtain a biomimetic movement, and a single stiffness value is sufficient for the knee and hip joints. According to Shamaei's suggestion, we decided to design variable stiffness actuator for ankle joint and series elastic actuators for knee and hip joints. Fig. 1 shows the CAD design of these actuators. Detailed explanations about BioComEx and its joint designs are presented in the relevant studies [40, 41].

2.1 Integration of MR brakes to BioComEx

MR brakes are electromagnetic structures that provide controllable damping torque with relatively small volume. In MR brakes, when MR fluid is exposed to a magnetic field, its shear stress changes and torque increases. According to the literature, multi-pole MR brake designs are superior designs with highest torque/volume ratio. Therefore, Baser et al. developed a 225-winding 4-pole MR brake to obtain a compact design and optimum torque performance [26]. Fig. 2 shows this 4-pole MR brake, its CAD section view, magnetic field strength and torque-current graph. As shown in Fig. 2(d), the torque provided by MR brake versus the applied current has some nonlinearity due to the hysteresis behavior of the ferromagnetic brake materials during charging and discharging period. Also, the brake has 0.3 Nm off-state torque. The time response of the bake is 50 ms. Table 1 shows the properties of MR brake.

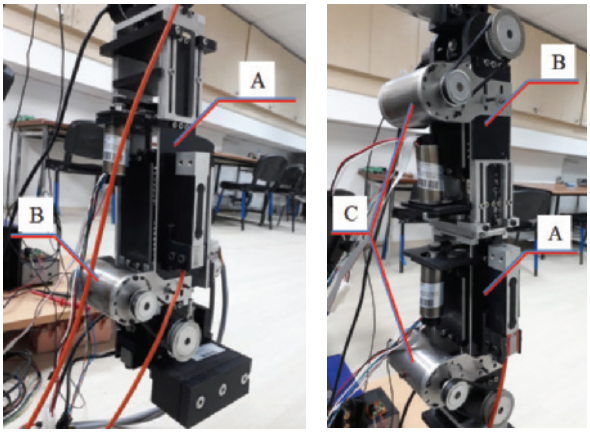

Fig. 3. Integration of MR brakes into the joints of BioComEx: (a) Ankle joint (A. Variable stiffness actuator, B. MR brake); (b) the knee and the hip joints (A-B. SEAs for the knee and the hip, C. MR brakes).

Although compliant actuators that drive BioComEx's joints provide biomimetic mobility, they are not sufficient for stable movement. To ensure a stable movement, 4-pole MR brakes were integrated into BioComEx joints via a timing belt drive system. Thus, variable impedance (stiffness/damping) hybrid actuator was created for all joints. Fig. 3 shows the integration of MR brakes into BioComEx joints. Adding braking property to the control system would enhance overall performance, since the MR brake is a kind of variable damping device that dissipates excess kinetic energy when it is activated.

3. Control algorithm architecture

Since BioComEx will be used for walking assistance, position control is required in all the joints. Fig. 4 shows the block diagram of the proposed control algorithm for the variable impedance actuator in the ankle joint. This control structure consists of three parts: Stiffness adjustment mechanism position control, VSA joint position control, and MR brake control. To track the position reference of the VSA, a PID position controller is used in the block diagram. Internal speed controller (G_{vel}) corresponds to the controller in the motor driver and ensures that the motor accurately tracks the speed command generated by the PID. However, large-scale oscillations are inevitable in the classical PID control of compliant actuators. To minimize these oscillations, the MR brake needs to be activated as a damping torque source during the operation. For MR brake activation, the derivative of the position control error is multiplied by another D parameter. Hence, minimum oscillating position control is achieved by a PID+D controller in BioComEx ankle joint. In addition, another PID control algorithm in the block diagram is

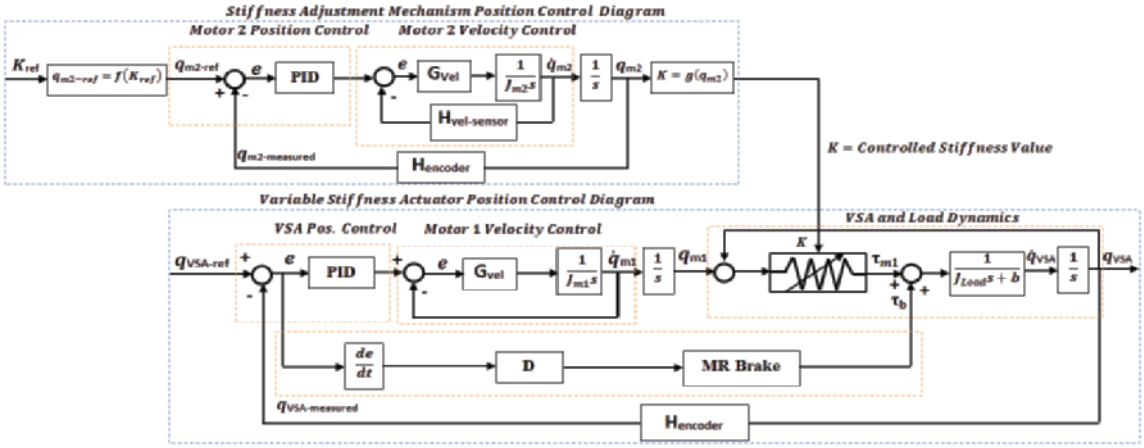

Fig. 4. Position control block diagram for ankle joint of BioComEx (position control block diagram for knee and hip joints are the same with ankle joint except for the part of stiffness adjustment mechanism).

applied for the stiffness adjustment motor.

The position control architecture of knee and hip joints of BioComEx is the same as the control architecture of ankle joint except for the position control of stiffness adjustment mechanism, which is shown in Fig. 4. The knee and hip joints in BioComEx are driven by series elastic actuators. Since the series elastic actuator is a compliant actuator with a constant spring coefficient, the control architecture does not have a stiffness adjustment motor. Similar to the control of ankle joint, the PID+D controller was employed for knee and hip joints as well: PID part of the PID+D control algorithm controls the position of series elastic actuator while D controller controls the MR brake damping torque. Thus, a more stable mobility is achieved in BioComEx knee and hip joints as well.

4. Experiments, results and discussion

To evaluate the proposed PID+D controller and hybrid actuators, some position control experiments were performed on BioComEx. In the experiments, two different implementations were conducted. First, position control algorithms were applied on each joint of BioComEx without a user and the results were presented separately for each joint. These experiments were also carried out against externally applied disturbing forces. In the secondary experiments, a hemiplegia patient having unilateral lower extremity disorders was considered. Thus, the performance of the variable impedance actuators and proposed PID+D control algorithm was examined on a device user. In the experiments with a device user, the position trajectories of user's healthy leg joints were captured with force feedback impedance control algorithm, and then these trajectories were used with a walking time delay as reference signal for the joints of the diseased leg. In the following sub-sections the achieved test results are presented in detail.

4.1 Position control experiments without user

In the experiments without a device user, the BioComEx leg was hung from the hip to a platform. Fig. 5 shows the test setup consisting of a variable impedance (stiffness/damping) ankle joint and knee and hip actuators with SEA and MR brake combination. This experimental setup can be considered as a three-limb pendulum.

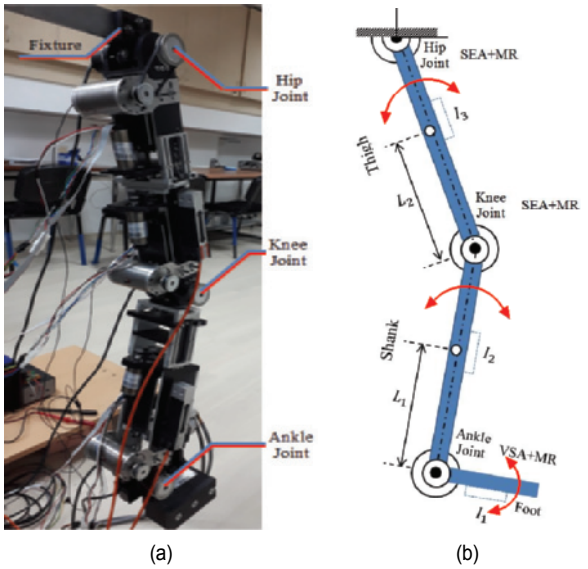

(a) (b)

Fig. 5. (a) Experimental setup used for the position control experiment of BioComEx with MR brakes; (b) schematic view of the load cell connection.

The most important point in this control architecture is the optimal adjustment of PID parameters. As is known, the Ziegler-Nichols method is the most preferred method for determining PID parameters in experimental studies. However, in this method the step response of the system overshoots and the rise time is very low, i.e., the system response is very fast. This situation is not suitable for safety in human-robot interaction studies. Because the exoskeleton robots are always exposed to sudden disturbing effects, fast response may destabilize the system under disturbances and put the user's safety at risk. In this study, instead of the Ziegler-Nichols method, a different

controller design criterion was considered in order to adjust PID parameters for human safety. PID parameters in this study were experimentally adjusted in such a way that the response of the system does not overshoot and rising time (t_r) is between 0.7 s and 0.8 s (0.7 s < t_r <0.8 s). Even in this case, when the compliant joints are exposed to external disturbing forces, significant oscillations are observed. For the elimination of these oscillations in the compliant joints, the derivative of the position error is multiplied by a parameter D to generate a damping torque reference for MR brake; in this way, the oscillation effects in the compliant actuators are considerably minimized.

The ankle joint has the property of variable stiffness. This changes the damping ratio of the system and distance of system poles from the imaginary axis of the complex plane. According to this, a sliding PID control logic was used to relocate the poles of the closed loop system relatively far from the imaginary axis of the complex plane for varying joint stiffness; in this way, the stability was guaranteed. This control embodiment can be described as follows; first, the stiffness values of the ankle joint are adjusted to three different values as low, medium and hard (200 Nm/rad, 450 Nm/rad and 900 Nm/rad, respectively), and these PID parameters are tuned in these three different stiffness values. These PID parameters are plotted versus ankle stiffness in a graph and line fittings are applied on these values. The PID parameters for the different stiffness values and the basic fitting lines on these values are shown in Fig. 6. Now, when the ankle stiffness is changed, PID parameters of the system are also changing along these lines.

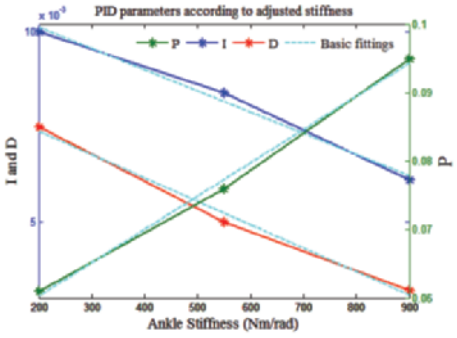

Fig. 6. Sliding P, I and D parameters during variable ankle stiffness.

In the step response experiments, steps of 20, 30 and 25 degrees were selected for the ankle, knee and hip joints, respectively. The joints sweep these angles approximately in 0.7-0.8 s at medium walking speed. Therefore, the design criterion of the rise time between 0.7-0.8 s without overshooting was considered in PID tuning of the system. Fig. 7 shows the results of step response experiments with PID according to Ziegler-Nichols method, PID according to the criterion of rise time of 0.7-0.8 s without overshooting, and PID+D controller with same criteria and MR brake activated. As shown in the figure, since there is no external load on the ankle joint, the ankle actuator is able to track the reference properly. The main effect of MR brake in ankle joint will appear in the experiments in which external forces are applied. However, the hip and knee joints show significant oscillations without MR brake due to thigh and shank weights. With the activation of MR brake, PID+D control algorithm makes the step responses of the knee and hip joints less oscillating.

In the rest of this section, position tracking experiments of the proposed control algorithm were conducted under external forces. I_1, I_2 and I_3 in Fig. 5 are the points of contact between the user and the robot. BioComEx was adapted to the user through the force sensors at these locations. The interaction forces were measured by these force sensors. In these experiments, the sinusoidal reference trajectories were given to the joints of BioComEx and random disturbing forces were applied during the operations. Fig. 8 shows the results of sinu-

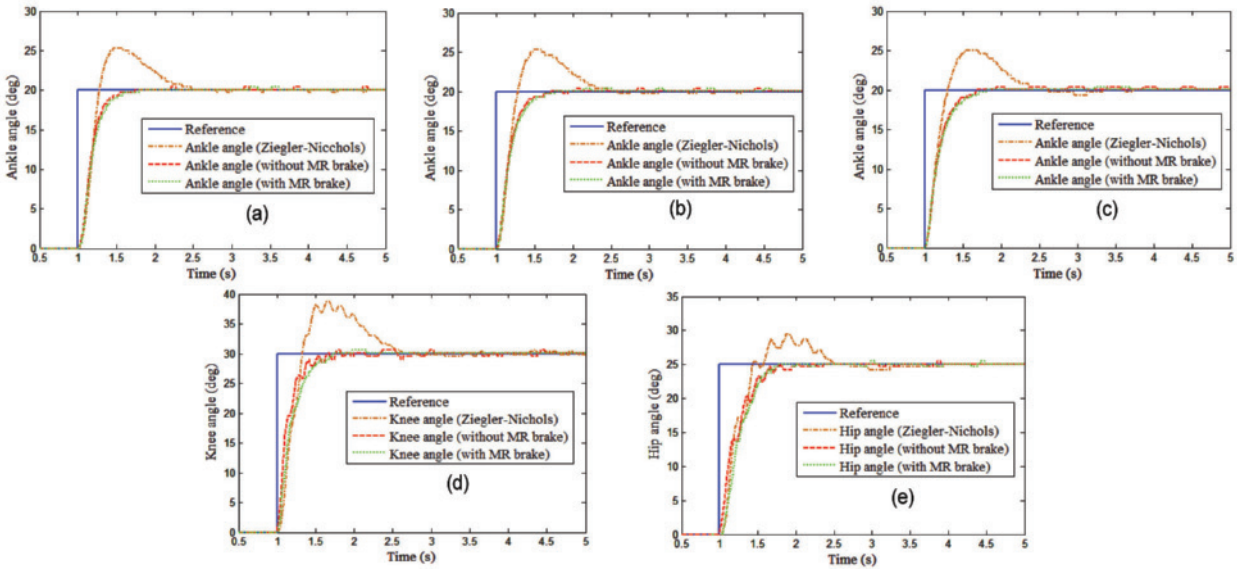

Fig. 7. (a) Step response results for ankle joint at high stiffness; (b) ankle joint at medium stiffness; (c) ankle joint at low stiffness; (d) knee; (e) hip joints.

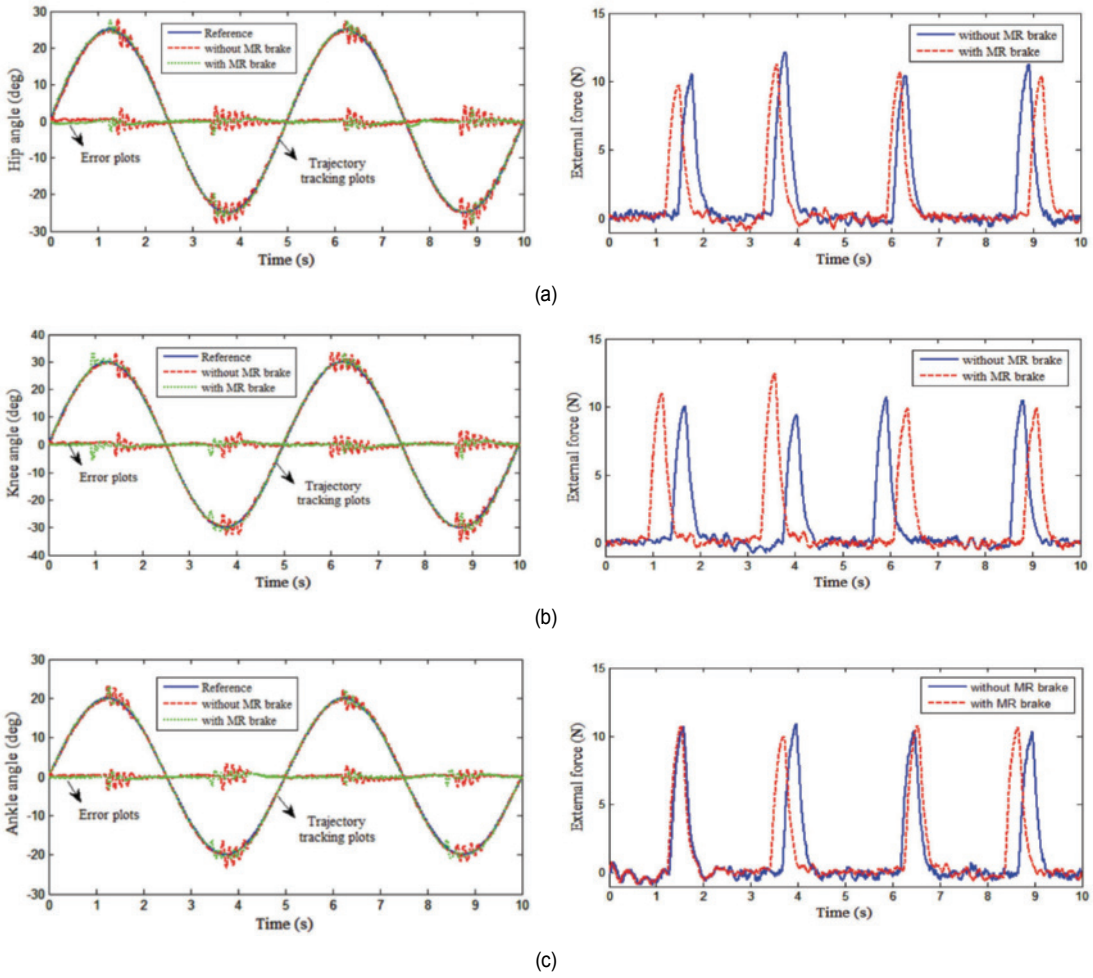

Fig. 8. Results of sinusoidal trajectory tracking experiments with external disturbance forces: (a) Ankle; (b) knee; (c) hip joints.

soidal trajectory tracking experiments with external disturbance forces. As shown, with PID controller without MR brake, due to the applied force, the joints deviate from the reference and a large number of oscillations occur until they seat on the reference again. However, with the PID+D controller combined with MR brake, the joints can quickly follow the reference with fewer oscillations. The oscillating effect of the disturbance forces on the position tracking is dissipated quickly by the damping property of MR brake. This clearly demonstrates the effectiveness of PID+D control algorithm with MR brake. It is important to note that the external forces were applied manually at the same level in each experiment.

4.2 Position control experiments with user

The lower limb exoskeleton robots are used to rehabilitate and assist the walking of patients. One of the techniques for the rehabilitation and assistance is to guide the walking of the impaired leg depending on a predefined gait trajectory. However, the predefined gait trajectory is not suitable for unilateral lower extremity disorders such as hemiplegia, since the predefined walking trajectory of the impaired leg cannot be synchronized continuously with the healthy leg [42]. Therefore, a different control strategy for the patients with unilateral lower extremity disorders is required. In this section, by considering hemiplegia patients, the phase delayed walking trajectory of the healthy leg was used for the reference of impaired leg. The walking guidance experiments were carried out on a user whose one leg was considered healthy and the other was impaired. In this way, the performance of the variable impedance actuators and proposed PID+D control algorithm were examined on the impaired side. An experimental setup was built for these experiments. Fig. 9 shows this experimental platform and BioComEx adapted to the user. The platform consists of three parts: a user hanging mechanism for anti-gravity, a back and side robot support, and a treadmill.

The experiments were performed by employing the force feedback impedance control algorithm on the healthy leg joints and the proposed PID+D control algorithm applied on the impaired leg joints. During the experiments, the user was asked to move his right leg normally and release his left leg according to the robot movement and was allowed to get support via his arms from the parallel bars on the right and left sides to ensure balancing. The healthy side's movements were detected

through force sensors placed between BioComEx and the user, and the robot followed the motions of the user based on these sensor feedbacks in real time. Then, the measured positions of the healthy leg joints were used as reference signal for the joints of the impaired leg with 2 seconds delay. In the experiments, the treadmill was adjusted to a speed of 1 km/h (≈ 0.28 m/s). The delay between the healthy leg and the impaired leg was determined in accordance with this treadmill speed.

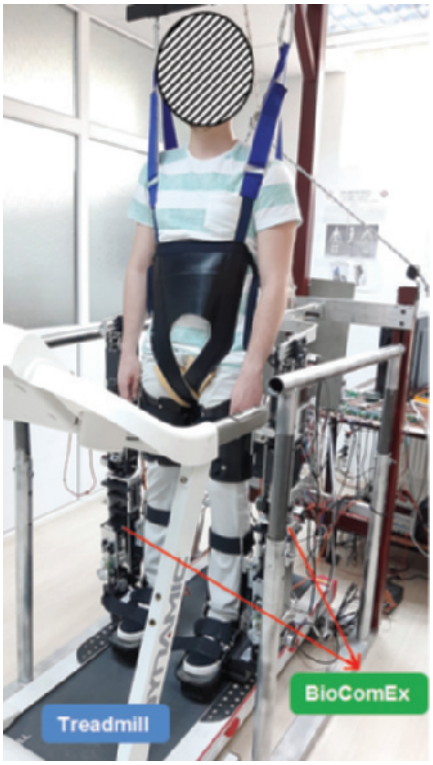

Fig. 9. Experimental setup of BioComEx with MR brakes on the user walking on the treadmill.

Fig. 10 shows the force feedback impedance control algorithm applied on the healthy joints. The robot follows the healthy leg by means of the force feedback control. In the meantime, the joint trajectories of the healthy leg were measured by encoders located on the robot. The impedance control algorithm for all joints is similar; the only difference is that the value of the stiffness comes from the stiffness adjustment mechanism in the variable stiffness actuator of ankle joint while it is constant in series elastic actuator of knee and hip joints. However, the stiffness of the variable stiffness actuators was set to a constant high value (900 Nm/rad) to simplify the tests. As shown in Fig. 10, the force feedback impedance control algorithm is multi-layered. The innermost loop is the motor velocity control loop and G_{vel} in this loop is the controller of motor driver. The middle loop is the torque feedback control loop and G_{torque} in this loop is a PID torque controller. P, I and D parameters of this controller were tuned by a step input response in such a way that 0.1 second rise time, % 10 maximum overshoot and % 2 steady state error were adjusted. The outermost loop is the impedance control loop and $G_{impedance}$ in this loop is the impedance model that is to be reflected to the user. In these experiments, the impedance model ($G_{impedance}$) was set to zero so that the robot could follow the user with minimum reaction. θ_{ref} in the block diagram denotes the user's healthy joints movement; it is measured by the encoders attached at link joints. A dashed feedback line was drawn to the outer of the control diagram for this purpose. The details of this force feedback impedance control algorithm are given in our previous study [25]. Since one contribution of the proposed study is the PID+D position control algorithm applied on the variable impedance exoskeleton joints, we concentrated on the position tracking performance of the impaired side. The experiment results of this PID+D position control algorithm applied on the impaired leg according the reference signal captured from healthy leg through the closed loop impedance

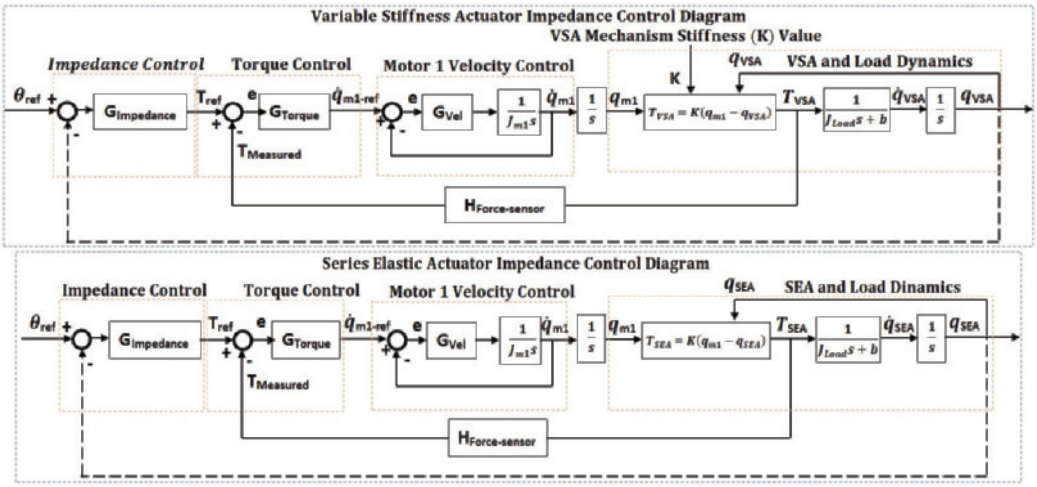

Fig. 10. Closed loop impedance control algorithm block diagram for variable stiffness actuator of ankle joint (top) and series elastic actuator of knee and hip joints (bottom).

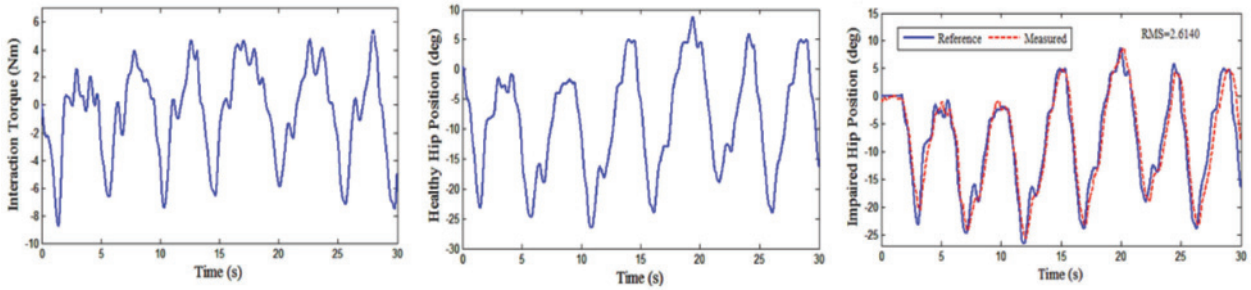

(a) (b) (c)

Fig. 11. (a) Interaction torque measured between the robot and healthy hip joint; (b) the measured position of the healthy hip joint; (c) the delayed reference position and measured position tracking of the impaired hip joint.

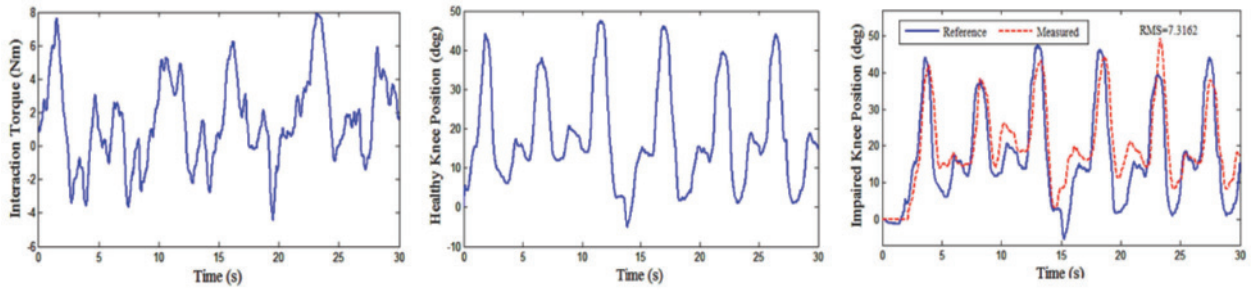

(a) (b) (c)

Fig. 12. (a) Interaction torque measured between the robot and healthy knee joint; (b) the measured position of the healthy knee joint; (c) the delayed reference position and measured position tracking of the impaired knee joint.

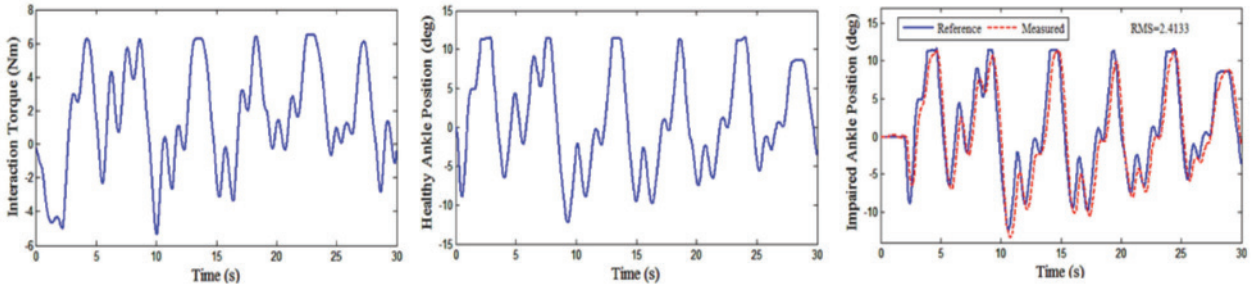

(a) (b) (c)

Fig. 13. (a) Interaction torque measured between the robot and healthy ankle joint; (b) the measured position of the healthy ankle joint; (c) the delayed reference position and measured position tracking of the impaired ankle joint.

control algorithm are given in Figs. 11-13. Each figure shows the interaction torque measured between the robot and healthy leg joints, the measured joint positions of the healthy leg, the delayed reference signals and the measured position tracking of the impaired leg joints. Some trajectory tracking errors like small phase shifts and fluctuations are seen in Figs. 11(c), 12(c) and 13(c) (position tracking RMS errors are given on the figures). These errors come from the nonlinearity of the system like hysteresis, time response, off-state torque of the MR brakes and stretch of timing belt drive system. However, high precision trajectory tracking as in the industrial robots is not needed in the exoskeletons. On the other hand, with the impedance control algorithm applied on healthy joints, the interaction torque between BioComEx and the user healthy leg ranges between ± 5-8 Nm. The experiments conducted in this section showed that while the closed loop impedance control algorithm helps the exoskeleton to trace the motions of the user's healthy leg joints at the very least resistance, the proposed PID+D control algorithm succeeds in position tracking of the impaired leg joints with minimal errors despite disturbances like ground reactions and leg weights.

Lastly, the algorithms in this study are depicted as a continuous-time controller, but these were applied by a digital controller. Homaeinezhad et al. [43] stated that executing a control

algorithm constructed in continuous-time basis in a discrete-time operating system may introduce the possibility of system instability, specifically in cases of system discontinuity, but the control inputs with sufficiently small sampling time minimize this possibility. In digital control design, the sample time should be at least a factor of 5-10 times of the system time constant, which is the time required for the system to reach 63.2 % of its steady-state step response; however, sampling times are often chosen to be several hundred times faster than the system time constant [44]. Accordingly, the sample time of the controllers was selected as 1 ms in this study, which is 250 times smaller than the time constant (250 ms) of BioComEx joints. Additionally, in order to find tolerable range of time delay where the system is stable, simplified transfer functions were estimated with different I/O time delays by using the input and output data given in Figs. 11(c)-13(c) via MATLAB System Identification Toolbox; then, the step responses of these estimated transfer functions were examined and it was concluded that the tolerable range of time delay where stability of system might be expected is 0.3 s in maximum.

5. Conclusions

A lower limb exoskeleton robot with compliant actuators and MR brakes in all joints was developed, and a PID+D position control algorithm was proposed for a safe human-robot interaction and more stable mobility. To examine this developed robot and proposed controller, two sets of experiments were conducted. The first were the trajectory tracking control experiments under some disturbances without device user. In these first experiments, the robot was hung on a platform and external disturbing forces were applied during the operation. The second was the experiments of walking assistance conducted with a device user who had unilateral lower extremity disorders. In these second experiments, the impedance control algorithm was used to capture the joint positions of the user's healthy leg, then these positions were used as reference signal for the impaired leg, and the proposed PID+D control algorithm was applied to track the position reference on the impaired leg. According to the results, it was concluded that: (1) The disturbing force effects and oscillations, which are the biggest problem of compliant actuators, can be reduced by the proposed PID+D controller and integration of MR brakes in the joints, (2) the motion of the user's healthy leg can be captured with minimal resistance through the force feedback impedance control algorithm and the impaired leg side can mimic the healthy leg effectively by means of the proposed system.

Acknowledgments

The authors thank the Scientific and Technological Research Council of Turkey for the financial support of a research project titled as "Design and Control of a Biomimetic Exoskeleton Robot" and numbered 213M297.

References

[1] D. Lim, W. Kim, H. Lee, H. Kim, K. Shin, T. Park, J. Lee and C. Han, Development of a lower extremity exoskeleton robot with a quasi-anthropomorphic design approach for load carriage, *IEEE/RSJ Int. Conf. Intell. Robot. Syst*. (2015) 5345-5350.

[2] S. K. Banala, S. K. Agrawal and J. P. Scholz, Active leg exoskeleton (ALEX) for gait rehabilitation of motor-impaired patients, *IEEE 10th International Conference on Rehabilitation Robotics* (2007) 401-407.

[3] R. J. Farris, H. A. Quintero and M. Goldfarb, Preliminary evaluation of a powered lower limb orthosis to aid walking in paraplegic individuals, *IEEE Transactions on Neural Systems and Rehabilitation Engineering*, 19 (6) (2011) 652-659.

[4] A. B. Zoss, H. Kazerooni and A. Chu, Biomechanical design of the Berkeley lower extremity exoskeleton (BLEEX), *IEEE/ASME Transactions Mechatronics*, 11 (2) (2006) 128-138.

[5] J. F. Veneman, R. Kruidhof, E. E. Hekman, R. Ekkelenkamp, E. H. Van Asseldonk and H. Van Der Kooij, Design and evaluation of the LOPES exoskeleton robot for interactive gait rehabilitation, *IEEE Transactions on Neural Systems and Rehabilitation Engineering*, 15 (3) (2007) 379-386.

[6] A. Tsukahara, R. Kawanishi, Y. Hasegawa and Y. Sankai, Sit-to-stand and stand-to-sit transfer support for complete paraplegic patients with robot suit HAL, *Advanced Robotics*, 24 (11) (2010) 1615-1638.

[7] D. Miranda-Linares, G. Alrezage and M. O. Tokhi, Control of lower limb exoskeleton for elderly assistance on basic mobility tasks, *19th International Conference on System Theory, Control and Computing* (2015) 441-446.

[8] N. Aliman, R. Ramli and S. M. Haris, Design and development of lower limb exoskeletons: A survey, *Robotics and Autonomous Systems*, 95 (2017) 102-116.

[9] W. Meng, Q. Liu, Z. Zhou, Q. Ai, B. Sheng and S. S. Xie, Recent development of mechanisms and control strategies for robot-assisted lower limb rehabilitation, *Mechatronics*, 31 (2015) 132-145.

[10] J. Li, S. Li, Y. Ke and S. Li, Safety design and performance analysis of humanoid rehabilitation robot with compliant joint, *Journal of Mechanical Science and Technology*, 33 (1) (2019) 357-366.

[11] G. A. Pratt and M. M. Williamson, Series elastic actuators, *EEE/RSJ International Conference on Intelligent Robots and Systems* (1995) 399-406.

[12] H. Kizilhan, O. Baser, E. Kilic and N. Ulusoy, Comparison of controllable transmission ratio type variable stiffness actuator with antagonistic and pre-tension type actuators for the joints exoskeleton robots, *12th International Conference on Informatics in Control, Automation and Robotics*, 2 (2015) 188-195.

[13] J. E. Pratt, B. T. Krupp, C. J. Morse and S. H. Collins, The RoboKnee: An exoskeleton for enhancing strength and endurance during walking, *Proc. of IEEE International Conference on Robotics and Automation,* 3 (2004) 2430-2435.

[14] H. K. Kwa, J. H. Noorden, M. Missel, T. Craig, J. E. Pratt and P. D. Neuhaus, Development of the IHMC mobility assist exoskeleton, *IEEE International Conference on Robotics and Automation* (2009) 2556-2562.

[15] H. Vallery, J. Veneman, E. Van Asseldonk, R. Ekkelenkamp, M. Buss and H. Van Der Kooij, Compliant actuation of rehabilitation robots, *Robotics & Automation Magazine*, 15 (3) (2008).

[16] J. F. Veneman, R. Ekkelenkamp, R. Kruidhof, F. C. van der Helm and H. van der Kooij, A series elastic-and bowden-cable-based actuation system for use as torque actuator in exoskeleton-type robots, *The International Journal of Robotics Research*, 25 (3) (2006) 261-281.

[17] M. Dežman and A. Gams, Rotatable cam-based variable-ratio lever compliant actuator for wearable devices, *Mechanism and Machine Theory*, 130 (2018) 508-522.

[18] R. V. Ham, B. Vanderborght, M. V. Damme, B. Verrelst and D. Lefeber, MACCEPA, the mechanically adjustable compliance and controllable equilibrium position actuator: Design and implementation in a biped robot, *Robotics and Autonomous Systems*, 55 (10) (2007) 961-768.

[19] M. Cestari, D. Sanz-Merodio, J. C. Arevalo and E. Garcia, ARES, a variable stiffness actuator with embedded force sensor for the ATLAS exoskeleton, *Industrial Robot: An International J.*, 41 (6) (2014) 518-526.

[20] P. Cherelle, V. Grosu, P. Beyl, A. Mathys, R. Van Ham, M. Van Damme and D. Lefeber, The MACCEPA actuation system as torque actuator in the gait rehabilitation robot ALTACRO, *3rd IEEE RAS & EMBS International Conference on Biomedical Robotics and Biomechatronics* (2010) 27-32.

[21] J. Zhu, Y. Wang, J. Jiang, B. Sun and H. Cao, Unidirectional variable stiffness hydraulic actuator for load-carrying knee exoskeleton, *International J of Advanced Robotic Systems*, 14 (1) (2017).

[22] M. Cestari, D. Sanz-Merodio, J. C. Arevalo and E. Garcia, An adjustable compliant joint for lower-limb exoskeletons, *ASME Transactions on Mechatronics,* 20 (2) (2015) 889-898.

[23] B. Ugurlu, C. Doppmann, M. Hamaya, P. Forni, T. Teramae, T. Noda and J. Morimoto, Variable ankle stiffness improves balance control: Experiments on a bipedal exoskeleton, *ASME Transactions on Mechatronics*, 21 (1) (2015) 79-87.

[24] A. Enoch, A. Sutas, S. I. Nakaoka and S. Vijayakumar, BLUE: A bipedal robot with variable stiffness and damping, *International Conference on Humanoid Robots* (2012) 487-494.

[25] O. Baser, H. Kizilhan and E. Kilic, Biomimetic compliant lower limb exoskeleton (BioComEx) and its experimental evaluation, *Journal of the Brazilian Society of Mechanical Sciences and Engineering*, 41 (5) (2019) 226.

[26] O. Baser and M. A. Demiray, Comparison of 4-pole with 225 coil-turns and 6-pole with 150 coil-turns multi-pole inner coil rotary MR brake designs, *International J. of Materials, Mechanics and Manufacturing* (2017) 5-3.

[27] M. Laffranchi, L. Chen, N. Kashiri, J. Lee, N. G. Tsagarakis and D. G. Caldwell, Development and control of a series elastic actuator equipped with a semi active friction damper for human friendly robots, *Robotics and Autonomous Systems*, 62 (12) (2014) 1827-1836.

[28] E. Garcia, J. C. Arevalo, G. Muñoz and P. Gonzalez-de-Santos, Combining series elastic actuation and magneto-rheological damping for the control of agile locomotion, *Robotics and Autonomous Systems*, 59 (10) (2011) 827-839.

[29] C. Zhao and L. Guo, On the capability of PID control for nonlinear uncertain systems, *IFAC Papers Online,* 50 (1) (2017) 1521-1526.

[30] B. Gonenc and H. Gurocak, Blending algorithm for position control with a hybrid actuator made of DC servomotor and brake, *Industrial Robot: An International J.*, 38 (5) (2011) 492-499.

[31] T. Nakamura, Y. Midorikawa and H. Tomori, Position and vibration control of variable rheological joints using artificial muscles and magneto-rheological brake, *International J. of Humanoid Robotics*, 8 (1) (2011) 205-222.

[32] D. A. Winter, *Biomechanics and Motor Control of Human Movement*, 4th ed., Wiley, New Jersey (2009).

[33] J. Perry, *Gait Analysis: Normal and Pathological Function*, New Jersey, SLACK, Inc. (2002).

[34] A. Hansen, D. Childress, S. Miff, S. Gard and K. Mesplay, The human ankle during walking: implications for design of biomimetic ankle prostheses, *J. of Biomechanics*, 37 (10) (2004) 1467-1474.

[35] W. H. Clark and J. R. Franz, Activation-dependent changes in soleus length-tension behavior augment ankle joint quasi-stiffness, *Journal of Applied Biomechanics*, 35 (2019) 182-189.

[36] S. Kuitunen, P. V. Komi and H. Kyröläinen, Knee and ankle joint stiffness in sprint running, *Medicine and Science in Sports and Exercise*, 34 (1) (2002) 166-173.

[37] K. Shamaei, G. S. Sawicki and A. M. Dollar, Estimation of quasi-stiffness and propulsive work of the human ankle in the stance phase of walking, *PLoS ONE,* 8 (3) (2013) e59935.

[38] K. Shamaei, G. S. Sawicki and A. M. Dollar, Estimation of quasi-stiffness of the human knee in the stance phase of walking, *PloS ONE,* 8 (3) (2013) e59993.

[39] K. Shamaei, G. S. Sawicki and A. M. Dollar, Estimation of quasi-stiffness of the human hip in the stance phase of walking, *PloS ONE,* 8 (12) (2013) e81841.

[40] O. Baser and H. Kizilhan, Mechanical design and preliminary tests of VS-AnkleExo, *J. of the Brazilian Society of Mechanical Sciences and Engineering*, 40 (9) (2018) 442.

[41] O. Baser, H. Kizilhan and E. Kilic, Mechanical design of a biomimetic compliant lower limb exoskeleton (BioComEx), *Autonomous Robot Systems and Competitions* (2016) 60-65.

[42] C. Zhang, G. Liu, C. Li, J. Zhao, H. Yu and Y. Zhu, Development of a lower limb rehabilitation exoskeleton based on real-time gait detection and gait tracking, *Advances in Mechanical Engineering*, 8 (1) (2016) 1-9.

[43] M. R. Homaeinezhad and S. Yaqubi, Discrete-time sliding-surface based control of parametrically uncertain nonlinear systems with unknown time-delay and inaccessible switching mode detection, *International J. of Control* (2019) 1-20.

[44] R. H. Bishop, *Mechatronic System Control, Logic, and Data Acquisition,* 2nd Ed., CRC Press (2007).

Ozgur Baser received the M.S. and Ph.D. from Middle East Technical University, Turkey, in 2006 and 2012, respectively, all in mechanical engineering. He is currently an Associate Professor of Mechanical Engineering at Suleyman Demirel University, Turkey. His research interests include control systems, exoskeleton robots, MR brakes and haptic devices.

Hasbi Kizilhan received the M.S. from Department of Mechanical Engineering of Süleyman Demirel University, Turkey, in 2015. He is currently a Research Assistant and studying for his Ph.D. at the same department and university. His research interests include robotics, exoskeleton robots and human-robot interaction.

Ergin Kilic received the M.S. and Ph.D. from Middle East Technical University, Turkey, in 2007 and 2012, respectively, all in mechanical engineering. He is currently an Associate Professor of Mechanical Engineering at Suleyman Demirel University, Turkey. His research interests include fuzzy-logic control, artificial neural networks, rehabilitation robots and EMG signal processing.